Screening of the Pandemic Response Box identifies anti-microsporidia compounds

Qingyuan Huang[1,2], Jie Chen[1], Guoqing Pan[1#], and Aaron W. Reinke[2#]

[1]State Key Laboratory of Resource Insects, Chongqing Key Laboratory of Microsporidia Infection and Control, Southwest University, Chongqing, China,

[2]Department of Molecular Genetics, University of Toronto, Toronto, ON, Canada

#Corresponding author

gqpan@swu.edu.cn

aaron.reinke@utoronto.ca

Abstract

Microsporidia are fungi obligate intracellular pathogens, which infect most animals and cause microsporidiosis. Despite the serious threat that microsporidia pose to humans and agricultural animals, few drugs are available for the treatment and control of microsporidia. To identify novel inhibitors, we took advantage of the model organism *Caenorhabditis elegans* infected with its natural microsporidian *Nematocida parisii*. We used this system to screen the Pandemic Response Box, a collection of 400 diverse compounds with known antimicrobial activity. After testing these compounds in a 96-well format at high (100 μM) and low (40 μM) concentrations, we identified four inhibitors that restored the ability of *C. elegans* to produce progeny in the presence of *N. parisii*. All four compounds reduced the pathogen load of both *N. parisii* and *Pancytospora epiphaga*, a *C. elegans*-infecting microsporidia related to human-infecting species. One of these compounds, a known inhibitor of a viral protease, MMV1006203, inhibited invasion and prevented the firing of spores. A bis-indole derivative, MMV1593539, decreased spore viability. An albendazole analog, MMV1782387, inhibited proliferation of *N. parisii*. We tested albendazole as well as 5 other analogs and observed that MMV1782387 was amongst the strongest inhibitors of *N. parisii* and displayed the least host toxicity. Our study further demonstrates the effectiveness of the *C. elegans-N. parisii* system for discovering microsporidia inhibitors and the compounds we identified provide potential scaffolds for anti-microsporidia drug development.

Introduction

Microsporidia are obligate intracellular pathogens phylogenetically related to the fungi [1, 2]. Approximately 1700 species of microsporidia have been identified to infect invertebrates, vertebrates, and protists, with at least 17 species known to infect humans [3-5]. In addition to posing a serious threat to human health, microsporidia are responsible for substantial economic losses in agriculture. Species of farmed penaeid shrimp are susceptible to hepatopancreatic microsporidiosis, which is caused by *Enterocytozoon hepatopenaei* [3]. *Nosema ceranae* and *Nosema apis* are a threat to the global beekeeping industry [6, 7]. A lethal pathogen, *Nosema bombycis*, causes heavy losses or even total culture failure in the silkworm industry [8]. Moreover, some species, such as *Ameson portunus* and *Enterospora nucleophila*, have been identified to infect farmed crabs and fish, respectively [9, 10]. Among immunocompromised individuals, *Enterocytozoon bieneusi* and *Encephalitozoon intestinalis* are the most common microsporidia infections in humans and are associated with diarrhea and systemic illness [11, 12]. In underdeveloped countries, up to 51% of HIV-infected individuals with diarrhea have microsporidia infection [13]. Infections with zoonotic microsporidia have been discovered in livestock, companion animals, and wildlife, which poses a risk to public health [14]. In recent decades, the NIAID and CDC have recognized that many of these species of microsporidia pose a threat to human health. Thus, microsporidia have been classified as Category B priority pathogens for biodefense research [15].

There are few effective therapeutic interventions available to treat microsporidia infections [16]. Albendazole is known to inhibit microtubule polymerization by binding beta-tubulin and is effective against a variety of parasites with little adverse effects in humans [17, 18]. In infections of *Encephalitozoon* spp., albendazole has been demonstrated to control microsporidiosis [19]. However, several studies have shown that albendazole has a limited effect on microsporidiosis caused by *E. bieneusi* and *Vittaforma cornea* and that these species encode beta-tubulin with substitutions associated with resistance [20-22]. Analogs of albendazole, benomyl, and carbendazim, have been used to control microsporidia in insects such as *Nosema heliothidis* in *Heliothis zea* and *Nosema kingi* in *Drosophila willistoni* [16, 23, 24]. However, microsporidiosis in mammals cannot be treated with benomyl and carbendazim because of their hepatotoxicity and toxic effects on reproduction [25, 26] [27]. Since benzimidazoles have been widely used for decades, resistance fears have arisen. Fumagillin binds specifically and covalently to methionine aminopeptidase type 2 (MetAP2) and can inhibit many species of microsporidia [28, 29]. However, due to concerns with host toxicity, this drug is not approved for use in humans [30]. Furthermore, fumagillin has been associated with concerns regarding its toxicity in agriculture applications [31]. Therefore, there is a need to identify additional anti-microsporidia inhibiting agents.

The model organism *Caenorhabditis elegans* has become a useful system in which to study microsporidia infections and to identify inhibitors. The first microsporidia reported to infect *C. elegans* was *Nematocida parisii* [32]. Infection of *C. elegans* by *N. parisii* begins when spores are ingested into the worm's intestinal lumen, where they expel their unique invasion apparatus called the polar tube [33]. This causes the sporoplasm to be deposited inside intestinal cells. The parasite then proliferates intracellularly as meronts and then differentiates into spores, which then exit into the intestinal lumen. Infection of *C. elegans* with *N. parisii* results in smaller body size, reduced reproductive fitness, and shortened life span [34-36]. This host-parasite system has become a model in which to study mechanisms of microsporidia invasion, proliferation, and spore exit [35, 37-39]. Other species of microsporidia have also been found to infect *C. elegans* including *Pancytospora epiphaga*, which is related to the human-infecting species *E. bieneusi* and *V. cornea* [40-42]. We recently described the use of *C. elegans* to screen compounds for activity towards *N. parisii* using a high-throughput 96-well based assay, resulting in the identification of inhibitors of microsporidia invasion and proliferation [4, 37, 43].

The Pandemic Response Box (PRB) is a promising source of anti-microsporidia compounds. Developed by the Medicines for Malaria Venture with the support of the Drugs for Neglected Disease Initiative, this is an open-access compound library consisting of 400 small molecule compounds that have antifungal, antibacterial and antiviral activity [44]. Compounds from this collection include those that can inhibit other types of parasites such as nematodes, amoebas, and the causative agent of malaria [45-47].

To identify novel microsporidia inhibitors, we screened the PRB using a modified version of our previously described *C. elegans*-*N. parisii* assay [43]. We screened this compound collection at two concentrations and identified four chemical inhibitors of microsporidia infection. We validated these compounds and additionally showed that all four compounds reduced the pathogen load of *N. parisii*. We then studied at what stage in the microsporidia life cycle each compound is active. We found that MMV1782387, an analog of albendazole, inhibits microsporidian proliferation. This compound, albendazole, and the other MMV compounds we identified also inhibit *P. epiphaga.* We also show that MMV1006203 inhibits spore firing and related flavone analogs also prevent *N. parisii* infection. Additionally, the viability of spores is decreased when they are treated with MMV1593539. Together our study identifies additional microsporidia inhibitors that can block microsporidia proliferation and invasion.

Material and Methods

97 *C. elegans maintenance*

98 The food source for *C. elegans*, *Escherichia coli* OP50-1, was grown to saturation in lysogeny
99 broth (LB) for 18 hours at 37°C. To generate animals for infection assays, the wild-type *C. elegans*
100 strain N2 was grown as a mixed population and L4 stage worms were picked onto 10 cm
101 nematode growth media (NGM) plates seeded with 10x OP50-1 *E. coli* and kept at 21°C for 4
102 days [48]. In order to synchronize the worms, M9 solution was used to remove the worms from
103 the NGM plates, sodium hypochlorite and sodium hydroxide were used to bleach them. Embryos
104 from gravid adults were released into the solution and after washing were incubated at 21°C for
105 18 to 24 hours until the embryos hatched.

106 *N. parisii spore preparation*

107 *N. parisii* (ERTm1) spores were prepared as described previously [36]. *C. elegans* N2 worms
108 were infected with *N. parisii* spores on NGM plates. Worms were incubated for several days to
109 generate a large population of infected worms, which were harvested and frozen at -80°C.
110 Zirconia beads (2 mm diameter) were used for mechanical disruption of the infected worms,
111 followed by the removal of embryos, larvae, and debris using a 5 µm filter (Millipore). *N. parisii*
112 spore preparations were confirmed to be free of contaminated bacteria and stored at -80°C. Spore
113 concentration was measured by counting DY96-stained spores using a sperm counting slide
114 (Cell-VU).

115 *Source of chemicals*

116 Medicines for Malaria Venture (MMV, Geneva, Switzerland) provided the PRB, which contains
117 compounds dissolved in 10 µL of DMSO at a concentration of 10 mM for inclusion. 2 µL of the
118 stock compounds were transferred to new plates containing 3 µL DMSO to generate 4 mM stocks.
119 For retesting, the individual solid compounds of MMV1006203, MMV1593539, MMV1634497 and
120 MMV1782387 were provided by the MMV. The analog compounds of albendazole, thiabendazole,
121 carbendazim, oxfendazole, mebendazole, fenbendazole, flavone and displurigen were purchased
122 from MilliporeSigma. Stocks of all compounds were stored at -80 °C.

123 *Phenotypic assays in 96-well plates to identify microsporidia inhibitors*

124 Previously described methods were adapted to quantify the ability of compounds to restore the
125 ability of *C. elegans* to produce progeny in the presence of *N. parisii* [43]. Each well of a 96-well
126 plate was filled with 25 µL of K-medium (51 mM NaCl, 32 mM KCl, 3 mM $CaCl_2$, 3 mM $MgSO_4$,
127 3.25 µM cholesterol) containing 5x OP-50 and *N. parisii* spores, with the exception of column 12

128 to which spores were not added. 25 µL of K-medium containing L1 worms was then added to
129 each well. 500 nL of compounds from the PRB were pinned into columns 2–11 using a 96-well
130 pinning tool manufactured by V&P Scientific. Additionally, 500 nL of DMSO was added to columns
131 1 and 12 for infected and uninfected controls, respectively. Each well contained 100 bleach-
132 synchronized L1 worms, 1% DMSO, 15,000 *N. parisii* spores/µL and 100 µM or 40 µM of
133 compounds. A breathable adhesive porous film was used to cover the 96-well plates, which were
134 placed inside humidity boxes wrapped in parafilm and incubated for 6 days at 21°C with shaking
135 at 180 rpm. Each compound was tested three times at both concentrations, with the exception of
136 17 compounds for which there was not sufficient amounts at which to test at 100 µM and 9
137 compounds for which there was not sufficient amounts at which to test at 40 µM (See S1 Data).

138 *Quantification of progeny production*

139 Following incubation, 10 µL of 0.3125 mg/mL Rose Bengal solution was added to each well using
140 an Integra VIAFLO 96 Electronic pipette. Plates were then wrapped in parafilm and incubated for
141 16–24 hours at 37 °C, resulting in magenta staining of the worms. 240 µL M9/0.1%Tween-20 was
142 added to each well and the plate and centrifuged for 1 minute at 2200 x g. 200 µL supernatant
143 was removed from each well and 150 µL of M9/0.1%Tween-20 was added to each well. Upon
144 mixing up the worms in the plate, 25 µL of the worms were transferred to 96-well white clear
145 bottom plates containing 300 µL M9/0.1%Tween-20. After 30 minutes, plates were scanned using
146 an Epson Perfection V850 Pro flat-bed scanner with the following settings: positive film-holder,
147 4800 dpi, and 24-bit color. In order to highlight stained worms, images were also modified using
148 GIMP version 2.8.18, with horizontal and vertical gridlines positioned such that each well is
149 separated by a grid and removing HTML color codes #000000 and #FFC9AF. Images were also
150 modified by applying unsharp masking with the following parameters (radius = 10, effect = 10,
151 threshold = 10). Hue saturation was adjusted by changing the lightness to 100 and the saturation
152 to -100 for yellow, blue, cyan, and green. For red and magenta, the lightness was changed to -
153 100 and the saturation to 100. Each well was exported as a single .tiff image using LZW
154 compression. MATLAB was used to run WorMachine [49] with the pixel binarization threshold set
155 to 30, the neighboring threshold to set to 1, and the maximum object area set toto 0.003%.

156 *Continuous infection assays*

157 24-well assay plate containing a total volume of 400 µL including 800 L1 worms and 15,000 *N.*
158 *parisii* spores/µL were used for continuous infection assays. Assays were performed for three
159 biological replicates using 100 µM of each compound except for dexrazoxane (60 µM). During the

160 incubation period, test plates were covered with breathable adhesive porous film, the boxes were
161 enclosed in parafilm, and the plates were incubated at 21 °C, with shaking at 180 rpm for four
162 days. Incubated samples were washed with M9/0.1%Tween-20, acetone-fixed, DY96-stained,
163 and analyzed by fluorescence microscopy.

164 *Pulse infection assays*

165 To generate infected worms, ~8000 bleach-synchronized L1 worms, 30 million *N. parisii* spores,
166 and 5 µL 10x OP50-1 were added to 6 cm NGM plates and incubated for three hours at 21 °C
167 after drying. To remove excess spores, the worms were washed twice with 5 mL M9/0.1%Tween-
168 20. Worms were then added to 24-well plates and set up as described in the continuous infection
169 assays, with the exception that no spores were added. For each of the biological replicates, three
170 wells were assayed for each compound. After incubation for 2 or 4 days as described above,
171 samples were fixed in acetone and stained with DY96 and a FISH probe as described below.

172 *Spore firing assays*

173 Spores at a concentration of 30,000 spores/µL were incubated for 24 h at 21 °C with compounds
174 at a concentration of 200 µM, except for ZPCK was at 120 µM, and 2% DMSO. After being washed
175 three times with 1 mL K-medium, the spores were used in the 24-well assay plates as described
176 above. The final concentrations in these assays were 15,000 spores/ µL, 100 µM compounds
177 except ZPCK (60 µM), and 1% DMSO. Each compound was tested in three biological replicates
178 in all assays. Incubation was performed as described above and after 3 h, samples were fixed in
179 acetone, stained with FISH and DY96, and examined by fluorescence microscopy.

180 *Mortality assay*

181 *N. parisii* spores were incubated for 24 h at 21 °C with compounds at a concentration of 200 µM.
182 For the heat treatment control, spores were incubated at 100°C for 10 minutes. The spores were
183 washed twice with H_2O, resuspended in 100 µL of H_2O containing 2 mg/L Calcofluor White M2R
184 and 8 µM SYTOX Green nucleic acid stain, and incubated for 10 minutes at room temperature.
185 Spores were washed twice in H_2O, 2.5 µL of each mixture were spotted on slides containing 2%
186 agar. The mortality rate was determined by counting the percentage of calcofluor white stained
187 spores that contained SYTOX Green signal.

188 *DY96 staining, fluorescence in situ hybridization (FISH), and fluorescence microscopy*

189 To remove excess OP50, samples were washed twice in 1 mL M9/0.1%Tween-20. They were
190 fixed in 700 µL acetone for 15 minutes or 500 µL PFA solution (4% PFA, 1x PBS, 0.1% Tween-

191 20) for 30 minutes. Then, samples were washed twice in PBS/0.1%Tween-20. For DY96 staining,
192 500 µL DY96 staining solution (10 µg/µL DY96, 0.1% SDS in 1xPBS + 0.1% Tween-20) was
193 added and samples were rotated for 30 minutes. EverBrite™ Mounting Medium with DAPI was
194 then added to the samples. FISH was performed using the microB FISH probe for *N. parisii* 18S
195 rRNA (ctctcggcactccttcctg) conjugated to Cal Fluor Red 610 (LGC Biosearch Technologies) [32].
196 After washing with PBS/0.1%Tween-20, samples were incubated in hybridization buffer (900 mM
197 NaCl, 20 mM pH=8 Tris HCl, 0.01% SDS) containing 5 ng/µL FISH probe at 46 °C for 1-6 hours.
198 Samples were washed once with 1 mL wash buffer (50 mL hybridization buffer + 5 mM EDTA).
199 These samples were also stained with DY96 as described above, except with DY96 at 20 µg/µL.
200 Samples were imaged using a ZEISS Axio Imager 2 at 5x–63x magnification and images were
201 captured using Zeiss Zen 2.3. Gravid worms were defined as the proportion of animals containing
202 any number of embryos. Infected worms were defined as the proportion of animals displaying any
203 newly formed spores. Low infection was defined as spores present in less than one half of an
204 animal, moderate infection was defined as spore present in half of an animal, and high infection
205 was defined as spores present throughout both halves of an animal. L1 progeny of the parents
206 could be distinguished in size and were not included in these measurements.

207 *P. epiphaga infection assays*

208 *P. epiphaga* strain JUm1396 spores were prepared similar to as described above for *N. parisii*.
209 For infection experiments with *P. epiphaga*, 24-well assay plates were set up to contain a final
210 volume of 400 µL in K-medium, including 800 L1 worms and 80,000 *P. epiphaga* spores /µL. All
211 compounds were at a concentration of 100 µM, except for dexrazoxane which was used at 60
212 µM. The final concentration of DMSO was 1%. Plates were incubated as described above for four
213 days. The samples were fixed in 4% PFA and stained by the FISH probe specific to *P. epiphaga*
214 18S rRNA (CAL Fluor Red 610CTCTATACTGTGCGCACGG). Fluorescence microscopy and
215 quantification of FISH fluorescence were performed as described above.

216 *Statistical analyses*

217 The data were collected from three independent experiments with 3 biological repelicates and
218 analyzed by GraphPad Prism. The means between replicates were compared using either
219 Student's t-test or one-way ANOVA with post hoc correction.

220

221

222 **Results**

223 **Screen of Pandemic Response Box identifies 4 microsporidia inhibitors**

224 To identify compounds from the PRB which inhibit microsporidia infection, we adapted our
225 previously described 96-well infection assays [43]. Earliest larval (L1) stage of *C. elegans* were
226 incubated with *N. parisii* spores and compound in liquid for six days at 21°C. Host animals infected
227 with *N. parisii* produce a reduced number of offspring and compounds which inhibit microsporidia
228 can restore the ability of these animals to produce progeny. To quantify the number of offspring
229 produced when incubated with each compound, animals in each well were stained with rose
230 bengal, imaged with a flatbed scanner, and counted using WorMachine [49](see methods). Each
231 compound was screened in triplicate at a concentration of 100 μM. We identified six compounds
232 that resulted in progeny production in infected worms of 35-90% relative to the uninfected controls
233 (Fig 1A). These compounds also increased progeny production by 1.7-8.5-fold compared to
234 infected controls. Four of these compounds significantly improved the production of *C. elegans*
235 progeny in the presence of *N. parisii* (Fig 1B-1D). To determine the effect of the compound
236 collection at a lower concentration, we screened each compound at 40 μM. We observed three
237 compounds which increased progeny production over 3-5.3-fold more than infected controls and
238 to more than 13% of the uninfected controls (Fig 1E). Two of these compounds resulted in
239 significantly more progeny production at 40 μM and these two compounds were also observed to
240 be significant at 100 μM (Fig 1F and 1G). In total we identified four compounds with significant
241 activity which we validated and characterized in subsequent experiments (Fig 1H).

242 We next sought to determine whether the four compounds which significantly restored *C. elegans*
243 progeny production also limited *N. parisii* infection. We set up assays similar to our initial screen
244 by culturing L1 worms continuously with *N. parisii* spores in the presence of compounds in 24-
245 well plates. After four days, worms were fixed and then stained with direct yellow 96 (DY96), which
246 binds to chitin, a critical component of *N. parisii* spore walls and *C. elegans* embryos (Fig 2A) [42,
247 50, 51]. In the presence of *N. parisii* spores, all four compounds significantly increased the
248 proportion of adult worms containing embryos (Fig 2B), which is consistent with the results from
249 our initial screen. Treatment with the newly discovered compounds and the known microsporidia
250 inhibitor dexrazoxane significantly reduced animals displaying newly formed *N. parisii* spores,
251 except for MMV1593539 (Fig 2C) [43]. To determine if MMV1593539 had any impact on *N. parisii*
252 infection, we quantified the proportion of worms displaying a low, moderate, or high infection level
253 (See methods) (Fig 2D-2F). Under these infection conditions, ~90 percent of control worms
254 displayed high infection levels and all four compounds significantly lowered infection (Fig 2F).

255 **MMV1782387 inhibits the proliferation of *N. parisii***

256 Inhibition of microsporidia infection could be achieved through two mechanisms. One, by
257 preventing microsporidia from invading cells, which could occur either through the inactivation of
258 spores or by prevent spores from germinating. Two, acting after invasion to reduce proliferation.
259 To test whether compounds limited proliferation, we set up pulse-chase experiments where we
260 infected worms for three hours, washed away excess spores, and then incubated the worms with
261 one of the four MMV compounds or with dexrazoxane which was previously shown to limit *N.*
262 *parisii* proliferation (Fig 3A) [43]. Treatment with MMV1782387 and dexrazoxane increased the
263 gravidity of worms (Fig 3B). Treatment with MMV1782387 also inhibited *N. parisii* proliferation
264 with 26.7% of worms having newly formed spores, which is less inhibition than was observed with
265 dexrazoxane (0.89%) (Fig 3C).

266 To determine whether MMV1782387 inhibits *N. parisii* by slowing proliferation or enhancing
267 parasite clearance, we examined pulse-chase infected animals at either 2 day (before spore
268 formation) or 4 days (after spore formation) post infection with probes specific for *N. parisii* 18S
269 rRNA [32]. Dexrazoxane was previously shown to significantly reduce the pathogen burden within
270 animals, without influencing the proportion of infected animals [43]. We observed that
271 MMV1782387, similar to dexrazoxane, did not cause a reduction in infected animals, but
272 significantly reduced the amount of meronts in the worms (Fig 3D-3F). None of the other MMV
273 compounds we tested reduced pathogen load of the worms at either 2- or 4-days post treatment.
274 Dexrazoxane also caused significantly more reduction in pathogen levels compared to
275 MMV1782387 (Fig 3E and 3F). Together our results show MMV1782387 inhibits microsporidia
276 proliferation but does not enhance parasite clearance.

277

278 ***N. parisii* spore firing is inhibited by MMV1006203**

279 The initial step of microsporidia invasion is spore germination. Many microsporidia, including *N.*
280 *parisii*, germinate (also called spore firing) in the intestinal lumen to initiate infection [32, 52, 53].
281 In order to determine whether any compounds reduce germination, we conducted spore firing
282 assays using the four MMV compounds as well as ZPCK, which has previously been shown to
283 inhibit spore germination [43]. *N. parisii* spores were incubated with compounds for 24 hours and
284 the spores were then washed to remove the compounds. These spores were then cultured with
285 *C. elegans* at the L1 stage for three hours and stained with FISH to visualize the sporoplasms
286 and DY96 to visualize the spores. Spore firing was determined by counting the number of spores

287 that did not contain a sporoplasm divided by the total number of spores. ZPCK and one of the
288 MMV compounds, MMV1006203, significantly reduced the spore firing rate (Fig 4A). All of the
289 compounds, as well as ZPCK, also significantly reduced the number of sporoplasms that had
290 invaded each worm (Fig 4B).

291 **_N. parisii_ spores are inactivated by MMV1593539**

292 One way that microsporidia infection could be prevented is through the inactivation of
293 microsporidia spores. To test whether any of the MMV compounds inactivated the spores, we
294 performed mortality assays. Compounds were incubated with *N. parisii* spores for 24 hours and
295 then stained with calcofluor white, a dye that binds to spore wall, and SYTOX Green, a dye that
296 stains the nucleus of inviable cells. We then counted the number of spores that were inviable,
297 using heat treatment as a control for maximum spore inactivation. One of the MMV compounds,
298 MMV1593539, significantly increased, mortality rates, though not to the same extent as heat
299 treatment (Fig 4C).

300 **Benzimidazole and flavone analogs inhibit _N. parisii_ infection**

301 The benzimidazole molecule albendazole is one of the main treatment options currently used for
302 microsporidia infection. The structure of MMV1782387 is similar to albendazole and the PRB
303 contains several other benzimidazoles including carbendazim, fenbendazole, and oxfendazole.
304 However, these other benzimidazole compounds were not identified in our initial screen. We first
305 tested whether MMV1782387 and six benzimidazole analogs reduced the reproductive fitness of
306 uninfected *C. elegans* (Fig 5G). At 40 μM, there is no difference in the percentage of worms
307 forming embryos when treated with any of the compounds (Fig 5A). In contrast, menbendazole
308 and oxfenfazole significantly reduced progeny production in uninfected animals at 100 μM,
309 indicating moderate toxicity to the host (Fig 5D). We then tested whether these benzimidazole
310 compounds could restore the formation of embryos in animals infected with *N. parisii* using our
311 continuous infection assays. Except thiabendazole, all of the compounds increased the
312 percentage of gravid worms in the presence of *N. parisii* at 40 μM (Fig 5B). At 100 μM,
313 MMV1782387, albendazole, and carbendazim increased the percentage of gravid worms with *N.*
314 *parisii* (Fig E). MMV1782387-treated worms displayed the largest increase in the percentage of
315 gravid worms. We also examined the percentage of worms with newly formed spores when
316 treated with these compounds. Except thiabendazole, all compounds displayed a reduction in
317 infected animals at 40 μM (Fig 5C). All compounds displayed a reduction in infected animals at
318 100 μM, with MMV1782387 displaying amongst the strongest inhibition of infection (Fig 5F).

319 These results suggest that benzimidazoles can inhibit *N. parisii* and that MMV1782387 shows
320 both strong inhibition of *N. parisii* as well as low host toxicity in *C. elegans*.

321 The compound we identified which inhibits spore firing, MMV1006203, has a structure similar to
322 flavone. To test whether flavone and an analog of MMV1006203, displurigen, could inhibit *N.*
323 *parisii*, we tested these compounds in continuous infection assays at a concentration of 40 μM or
324 100 μM (Fig 5L). All three of these compounds significantly increased the proportion of gravid
325 worms and reduced infection rates at a concentration of 40 μM (Fig 5H and 5I). At a concentration
326 of 100 μM, all three molecules were effective at inhibiting microsporidia infection, though only
327 MMV1006203 could significantly increase the gravidity of worms (Fig 5J and 5K). These results
328 show that molecules based on a flavone structure can inhibit *N. parisii* infection.

329

330 **Identified MMV compounds inhibit *P. epiphaga***

331 To test whether the four MMV compounds we identified were effective against other microsporidia
332 species, we tested them against *P. epiphaga.* This species of microsporidia infects the
333 hypodermis and muscle of *C. elegans* and belongs to the *Enterocytozoonida* clade, along with
334 the human pathogens *V. cornea* and *E. bieneusi* [40, 42]. In order to examine whether the four
335 inhibitors we identified from the PRB could inhibit *P. epiphaga* infection of *C. elegans*, we used
336 FISH staining to quantify the pathogen load. All of the compounds significantly reduced *P.*
337 *epiphaga* infection levels (Fig 6A). We tested albendazole against *P. epiphaga* and observed that
338 this compound also inhibited infection (Fig 6B).

339

340 **Discussion**

341 We screened the open-access PRB compound library, identifying four compounds with anti-
342 microsporidia activity. We quantified the ability of compounds to reproducibly alleviate the
343 reduction in *C. elegans* progeny caused by *N. parisii* infection. We validated all four compounds
344 identified from the initial screen, which is an improvement over our previous screen where we
345 qualitatively determined the effect of compounds from a single replicate and only about half of the
346 initially identified compounds were validated [43]. We show that the compounds we identified
347 have different effects on microsporidia, with MMV1782387 preventing proliferation, MMV1006203
348 preventing spore firing, and MMV1593539 causing an increase in spore mortality. When used to
349 treat spores, all four compounds inhibit invasion, though it is not clear why MMV1634491 and

350 MMV1782387 reduce sporoplasm numbers. It appears that these compounds limit microsporidia
351 invasion, but through some mechanism that will require additional experiments to determine. All
352 four compounds we identified in this study limited both *N. parisii* and *P. epiphaga* infection. These
353 results further demonstrate that *C. elegans* can be used to efficiently identify compounds with
354 activity against multiple species of microsporidia. One limitation of our approach is that inhibitors
355 that reduce the reproductive fitness of *C. elegans* on their own will not be observed. However,
356 this is also potentially beneficial as host toxicity, at least within the *C. elegans* context, is evaluated
357 at the same time as inhibition of microsporidia infection.

358 There is a range of bioactivity associated with benzimidazoles, including anti-inflammatory,
359 antihypertensive, anti-bacterial, anti-parasitic, and anti-fungal properties [16, 54-56]. The
360 benzimidazole albendazole is one of the most common treatments for microsporidia. Here we
361 show that MMV1782387, a benzimidazole carbamate, has amongst the strongest inhibition of *N.*
362 *parisii* and relatively low host toxicity in *C. elegans*. Benzimidazoles are known to inhibit *C.*
363 *elegans* and natural resistance to these compounds has arisen through genetic variation in beta-
364 tubulin [57, 58]. Host toxicity has been shown to be mediated through inhibition of neuronal beta-
365 tubulin [59]. Carbendazim, fenbendazole and oxfendazole are present in the PRB, however, in
366 our preliminary screening, we did not find that these compounds improved progeny production in
367 the presence of *N. parisii*. Beta-tubulin is the likely target of albendazole in microsporidia. *V.*
368 *cornea* and *E. bieneusi* contain a glutamine at position 198 in beta-tubulin that is associated with
369 albendazole resistance, and mutations in this position provide resistance in *C. elegans* [60]. *P.*
370 *epiphaga* beta-tubulin encodes for glutamate at this position which is associated with albendazole
371 sensitivity and is consistent with our data showing that this species can be inhibited by
372 benzimidazoles [21, 22, 41]. Given the similarity of the compounds, MMV1782387 may also inhibit
373 beta-tubulin. In compound library screens, multistage activity is one of the most preferred
374 attributes for molecules which inhibit pathogens [61]. We show that MMV1782387, which inhibits
375 proliferation of *N. parisii* can also reduce invasion by about 50%. MMV1782387 has been shown
376 to be effective against several fungal pathogens which cause eumycetoma and may have
377 potential for further development as an inhibitor of fungal pathogens [62].

378 Bis-indole analogs possess a broad range of pharmacological properties, including anti-cancer,
379 anti-bacterial, and anti-parasite properties [63, 64]. A type of bis-indole alkaloid, hamacanthin,
380 isolated from the sponge *Spongosorites* sp. demonstrated powerful antibacterial activity against
381 methicillin-resistant *Staphylococcus aureus* [65]. In addition to several antileishmanial scaffolds
382 reported, indole alkaloids showed promising activity against Leishmania parasites [66, 67].

383 Docking studies have shown that bisindole analogs are potent inhibitors of pteridine reductase
384 [64]. Here we found that dormant microsporidia spores can be inactivated in by MMV1593539, a
385 bis-indole derivative. We show that treatment of spores with MMV1593539 causes both a
386 decrease in viability and a decrease in sporoplasm invasion. Interestingly, MMV1593539 has
387 been reported to have anthelmintic activity against the parasitic nematode *Haemonchus contortus*,
388 but this compound is not active against *C. elegans* [45].

389 Microsporidia infect host cells through spore germination, and this process may be regulated by
390 receptor proteins on cell membranes and external signals [68, 69]. Furthermore, the changes in
391 calcium ion concentrations, osmotic pressure of the external medium, or *in vivo* host environments
392 can induce microsporidia spore firing [70-72]. However, many of the microsporidia proteins
393 involved in spore firing are unknown. The subtilisin-like protease NbSLP1 has been implicated in
394 germination as the active version localizes to the site of the spore where polar tube firing occurs
395 in *N. bombycis* spores [73] [74]. We previously found that protease inhibitors and quinones can
396 inhibit spore firing [43]. Here we show that MMV1006203, a flavone, can prevent microsporidia
397 invasion and spore firing. This inhibition occurs after incubation of the compound with spores,
398 followed by washing of the spores, suggesting that this inhibitor acts directly on the spores to
399 prevent firing. The molecular structures of displurigen and flavone are similar to that of
400 MMV1006203, and these compounds also display the ability to prevent *N. parisii* infection. Other
401 flavone compounds such as quercetin were shown to inhibit *Encephalitozoon intestinalis* infection,
402 but it was not determined if these compounds block microsporidia invasion [75]. MMV1006203
403 was first shown to inhibit the human cytomegalovirus (HCMV) protease and more recently to have
404 activity against *Plasmodium falciparum* [46, 76].

405

406 Further work will be necessary to determine the molecular target of MMV1006203 in preventing
407 microsporidia spore firing. Several approaches have been used in other eukaryotic intracellular
408 parasites to identify targets of inhibitors. On approach is evolving strains that are resistant to an
409 inhibitor and sequencing isolates to determine the genetic variants responsible for causing
410 resistance [77]. A complementary biochemical-based approach is to use thermal proteome
411 profiling to identify proteins which have a change in thermal stability upon addition of the inhibitor.
412 The efficacy and specificity of the compounds we have identified could also be further optimized
413 by characterizing a collection of closely related analogs, which has been done for fumagillin [78].

414

415

Acknowledgements

We are grateful to Winnie Zhao, Yin Chen Wan, Meng Xiao, Jonathan Tersigni, Hala Tamim El Jarkass, and Edward James for providing helpful comments on the manuscript. We thank the Medicines for Malaria Venture for providing the PRB compound library and the individual compounds to retest. **Funding:** This work was supported by Canadian Institutes of Health Research grant (no. 461807 to A. W. R.) and Q. H was supported by an award from the China Scholarship Council. **Competing interests:** The authors declare that they have no competing interests. **Data availability:** All data is presented in S1 Data.

426 **Figures and legends**

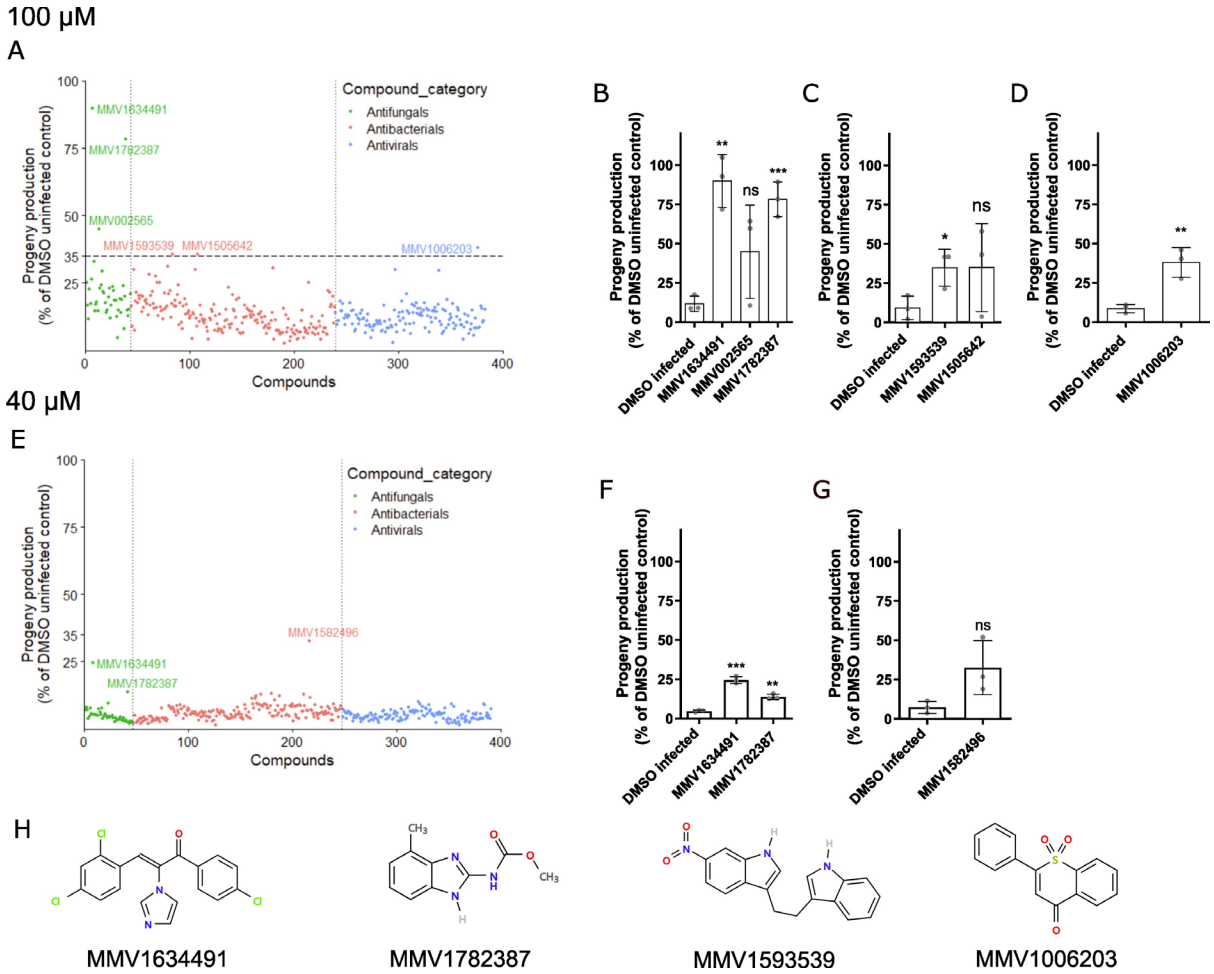

427 **Fig 1. Four compounds from the PRB restored *C. elegans* progeny production in the presence of *N. parisii*.** (A and E) Compounds at concentration of 100 µM (A) or 40 µM (E) were incubated with *C. elegans* and *N. parisii* for 6 days. Each point represents the mean progeny production of a compound expressed as the percentage of the DMSO uninfected control. The compound-ID is shown for compounds that had an activity of at least 35% (A) or ≥ 13% (E). Compounds are divided into their disease area as classified by the PRB and colored according to the legend at the right. 17 compounds in the collection were not screened at 100 µM and 9 compounds not screened at 40 µM due to lack of material (S1 Data). (B-D) Compounds that had an activity of at least 35% at 100 µM. (B) Antifungals, (C) Antibacterials, (D) Antivirals. (F and G) Compounds that had an activity ≥ 13% at 40 µM. (F) Antifungals, (G) Antibacterials. (H) The chemical structures of the four PRB compounds with significant activity. Statistical significance was determined by Student's t-test with comparisons to the DMSO infected control. Means ± SD (horizontal bars) are shown. (*$p < 0.05$, **$p < 0.01$, ***$p < 0.001$, ns means not significant).

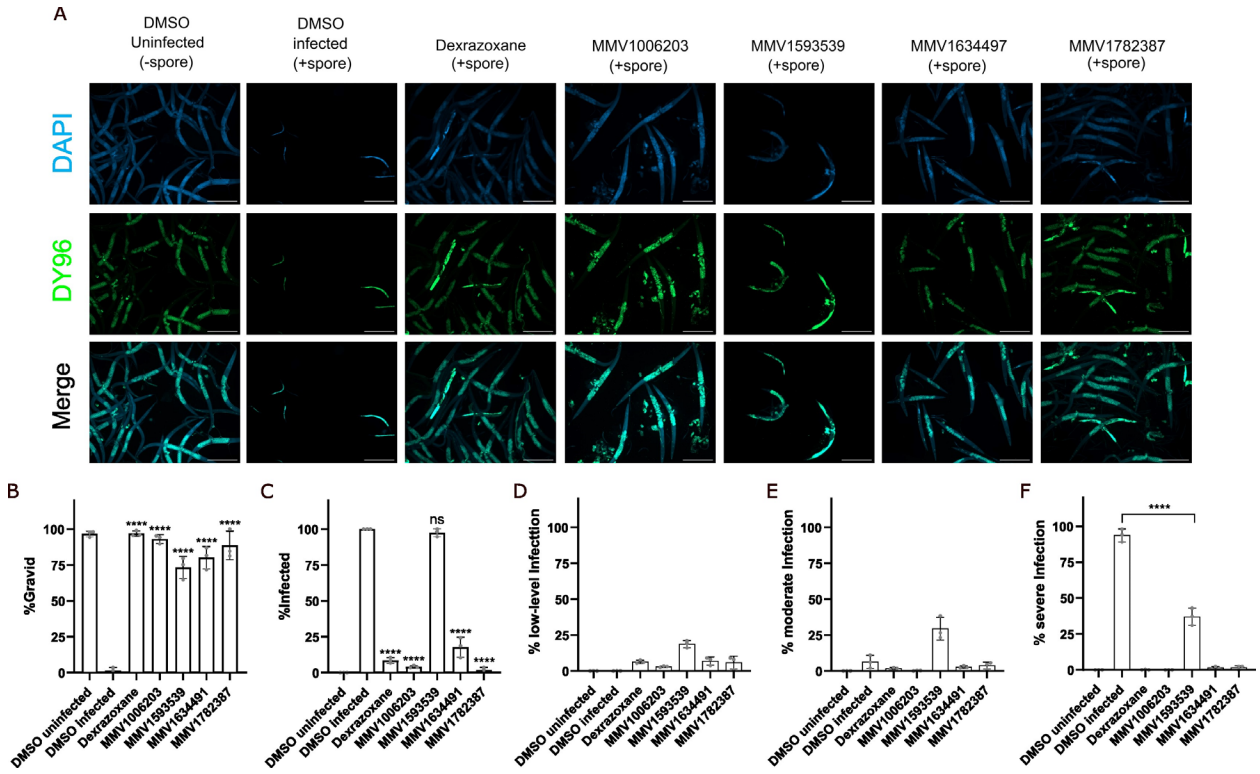

Fig 2. Identified MMV compounds inhibit *N. parisii*. (A-F) L1 stage animals with incubated in the presence of *N. parisii* spores and compounds for 4 days. Animals were then fixed and stained with DY96 and DAPI. (A) Representative images of continuous infection assays taken at a magnification of 50x; scale bars are 500 µm. (First and second columns) Worms incubated without (-spore) or with spores (+spore). As a result of microsporidia infection, fewer worms become gravid, and new spores are formed. Microsporidia spores and nematode embryos are stained green by DY96. (Third to seventh columns) Dexrazoxane and the identified PRB compounds inhibit spore formation and restore embryo production. (B) The percentage of worms with embryos (n = 3, N = ≥ 100 worms counted per biological replicate). (C) The percentage of worms with newly formed spores (n = 3, N = ≥ 100 worms counted per biological replicate). (D-F) The percentage of worms with (D) low-level infection, (E) moderate infection, and (F) severe infection. The P-values were determined by one-way ANOVA with post hoc test. Means ± SD (horizontal bars) are shown. (***$p < 0.001$, ****$p < 0.0001$, ns means not significant).

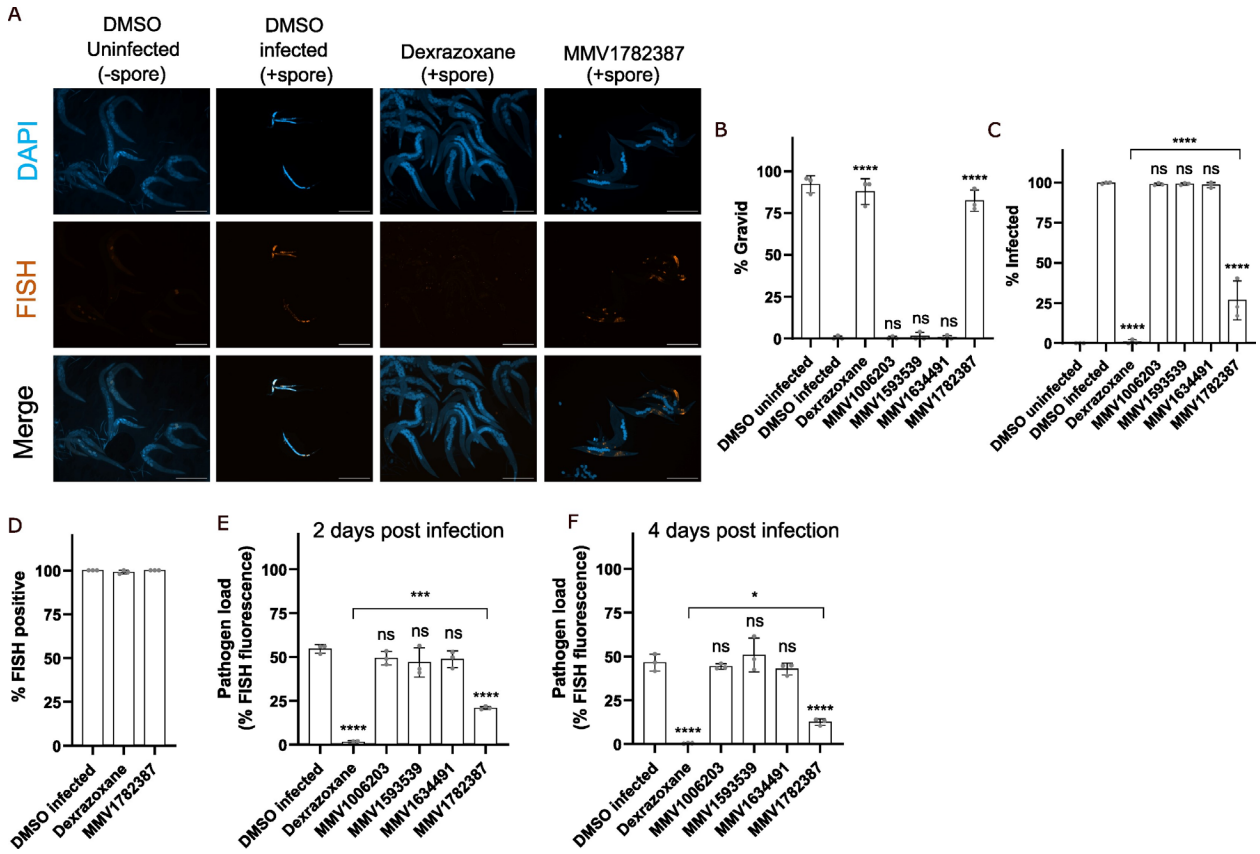

Fig 3. MMV1782387 inhibits microsporidia proliferation. (A-F) L1 stage animals were incubated in the presence of *N. parisii* spores for 3 hours and then washed to remove excess spores. Compounds were then added, and animals were incubated for 2 (E) or 4 (A-D and F) days, fixed, and stained with DY96, DAPI and a FISH probe specific to the *N. parisii* 18S rRNA. (A) Representative images of pulse infection assays taken at a magnification of 50x; scale bars are 500 μm. (First and second columns) Worms uninfected or infected with *N. parisii* spores. Sporoplasms and meronts are stained in red with FISH probes. (Third and fourth columns) Dexrazoxane or MMV1782387 treatment reduces *N. parisii* meronts. (B) The percentage of worms with embryos (n = 3, N = ≥ 100 worms counted per biological replicate). (C) The percentage of worms with newly formed spores (n = 3, N = ≥ 100 worms counted per biological replicate). (D) The percentage of worms with FISH signal (n = 3, N = ≥ 100 worms counted per biological replicate). (E and F) Quantitation of pathogen load (FISH fluorescence area %) per worm for (E) 2 or (F) 4 days post infection (n = 3, N = 10 animals quantified per biological replicate). The P-values were determined by one-way ANOVA with post hoc test. Means ± SD (horizontal bars) are shown. (*p <0.05, ***p < 0.001, ****p < 0.0001, ns means not significant).

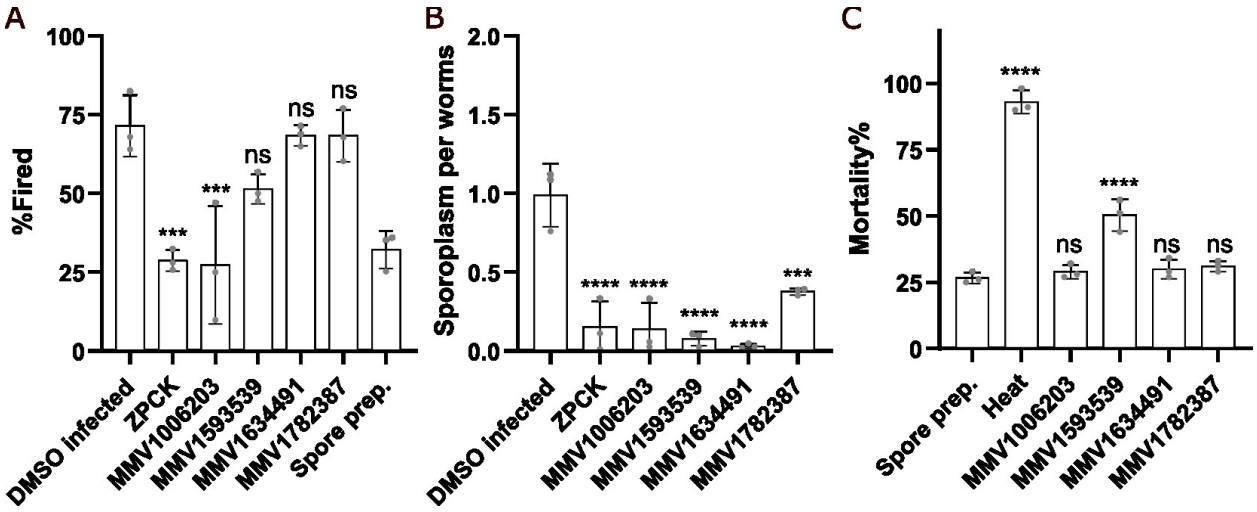

Fig 4. MMV1006203 inhibits spore firing *in vivo* and MMV1593539 inactivates spores *in vitro*. (A-B) *N. parisii* spores were incubated with compounds for 24 hours and then washed to remove compounds. Spores were then incubated with L1 stage worms for 3 hours, fixed, and stained with DY96 and *N. parisii* 18S rRNA FISH probe. (A) The percentage of fired spores in the intestinal lumen (n = 3, N = ≥ 50 spores counted per biological replicate). (B) The mean number of sporoplasms per worm (n = 3, N = ≥ 50 worms counted per biological replicate). (C) *N. parisii* spores were incubated with compounds for 24 hours and stained with SYTOX Green and Calcofluor White M2R. The percentage of spores that showed SYTOX Green staining (n=3, N= ≥ 100 spores counted per biological replicate). The P-values were determined by one-way ANOVA with post hoc test. Means ± SD (horizontal bars) are shown. (***$p < 0.001$, ****$p < 0.0001$, ns means not significant).

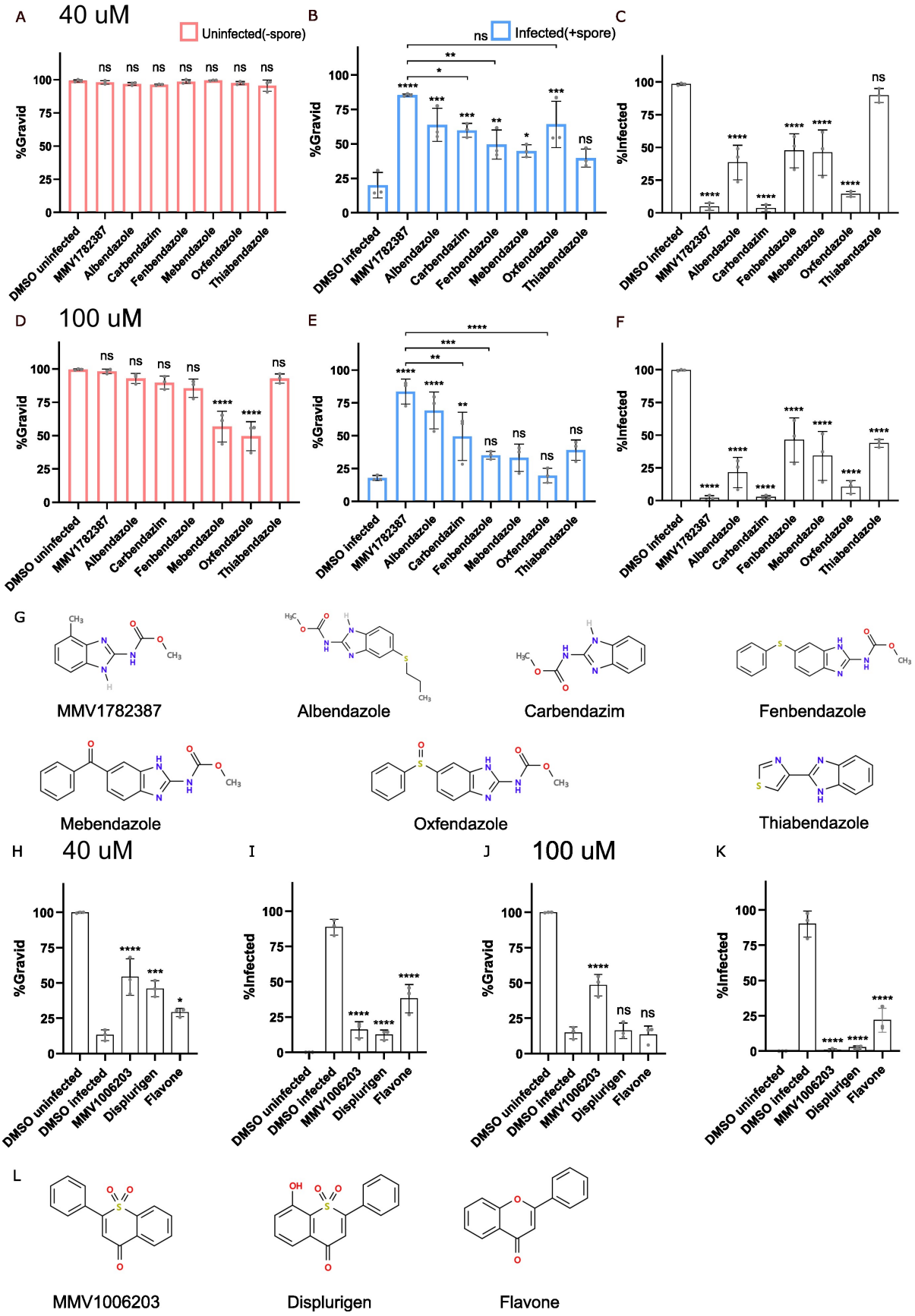
A
40 uM
Uninfected(-spore)
%Gravid
DMSO uninfected
MMV1782387
Albendazole
Carbendazim
Fenbendazole
Mebendazole
Oxfendazole
Thiabendazole
B
Infected(+spore)
C
%Infected
D
100 uM
E
F
G
MMV1782387
Albendazole
Carbendazim
Fenbendazole
Mebendazole
Oxfendazole
Thiabendazole
H
40 uM
I
J
100 uM
K
DMSO uninfected
DMSO infected
MMV1006203
Displurigen
Flavone
L
MMV1006203
Displurigen
Flavone

487 **Fig 5. Benzimidazole and flavone analogs limit *N. parisii* infection.** (A-F and H-K) L1 stage
488 animals were continuously incubated with *N. parisii* spores and indicated compounds for 4 days,
489 fixed, and stained with DY96 and DAPI. (A-F) Effect of benzimidazoles at 40 μM (A-C) or 100
490 μM (D-F) on the percentage of worms with embryos in uninfected worms (A and D), infected
491 worms (B and E) and the percentage of worms (C and F) with newly formed spores (n = 3, N =
492 ≥ 100 worms counted per biological replicate). (G) Chemical structures of benzimidazole
493 analogs. (H-K**)** Effect of flavones at 40 μM (H-I) or 100 μM (J-K) on the percentage of worms
494 with embryos (H and J) and the percentage of worms with newly formed spores (I and K) (n = 3,
495 N = ≥ 100 worms counted per biological replicate). (L) Chemical structures of flavone analogs.
496 The P-values were determined by one-way ANOVA with post hoc test. Means ± SD (horizontal
497 bars) are shown. (*p < 0.05, **p < 0.01, ***p < 0.001, ****p < 0.0001, ns means not significant).

498

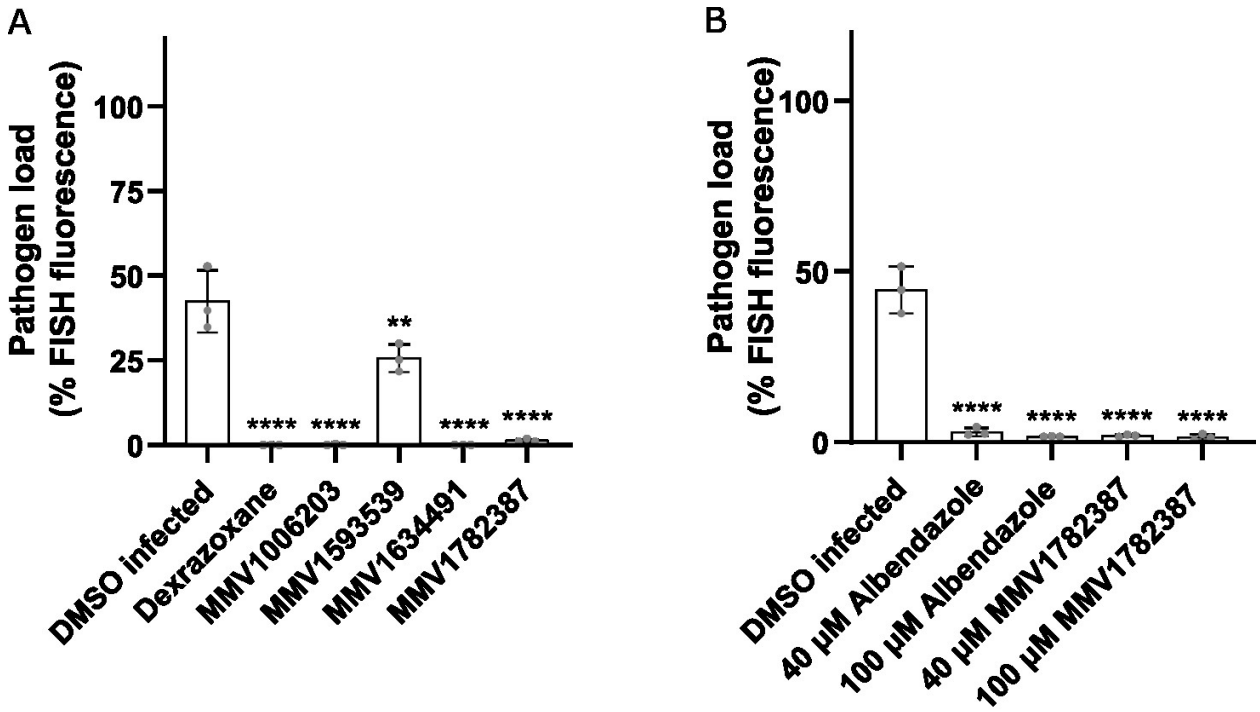

499

500 **Fig 6. *P. epiphaga* infection is impeded by the identified MMV inhibitors and albendazole.**
501 (A and B) L1 stage animals were continuously incubated with *P. epiphaga* spores for four days,
502 fixed, and stained with a *P. epiphaga* 18S rRNA FISH probe. Quantification of pathogen load
503 (%FISH fluorescence area) per worm 4 days post infection (n = 3, N = 10 animals quantified per
504 biological replicate). The P-values were determined by one-way ANOVA with post hoc test.
505 Means ± SD (horizontal bars) are shown. (*p < 0.05, **p < 0.01, ***p < 0.001).

506

507 **References**

508 1. Keeling PJPp. Five questions about microsporidia. 2009;5(9):e1000489.
509 2. Wadi L, Reinke AWJPp. Evolution of microsporidia: An extremely successful group of eukaryotic
510 intracellular parasites. 2020;16(2):e1008276.
511 3. Chaijarasphong T, Munkongwongsiri N, Stentiford GD, Aldama-Cano DJ, Thansa K, Flegel TW, et
512 al. The shrimp microsporidian Enterocytozoon hepatopenaei (EHP): Biology, pathology, diagnostics and
513 control. 2021;186:107458.
514 4. Han B, Takvorian PM, Weiss LMJFim. Invasion of host cells by microsporidia. 2020;11:172.
515 5. Murareanu BM, Sukhdeo R, Qu R, Jiang J, Reinke AWJM. Generation of a microsporidia species
516 attribute database and analysis of the extensive ecological and phenotypic diversity of microsporidia.
517 2021;12(3):10.1128/mbio. 01490-01421.
518 6. Higes M, Meana A, Bartolomé C, Botías C, Martín-Hernández RJEmr. N osema ceranae
519 (Microsporidia), a controversial 21st century honey bee pathogen. 2013;5(1):17-29.
520 7. Forsgren E, Fries IJVp. Comparative virulence of Nosema ceranae and Nosema apis in individual
521 European honey bees. 2010;170(3-4):212-217.
522 8. Bhat I, Buhroo Z, Bhat MJIJER. Microsporidiosis in silkworms with particular reference to
523 mulberry silkworm (Bombyx Mori L.). 2017;2(1):1-9.
524 9. Wang Y, Li X-C, Fu G, Zhao S, Chen Y, Wang H, et al. Morphology and phylogeny of Ameson
525 portunus n. sp.(Microsporidia) infecting the swimming crab Portunus trituberculatus from China.
526 2017;61:122-136.
527 10. Picard-Sánchez A, Piazzon MC, Ahmed NH, Del Pozo R, Sitjà-Bobadilla A, Palenzuela OJVP.
528 Enterospora nucleophila (Microsporidia) in gilthead sea bream (Sparus aurata): Pathological effects and
529 cellular immune response in natural infections. 2020;57(4):565-576.
530 11. Didier ESJAt. Microsporidiosis: an emerging and opportunistic infection in humans and animals.
531 2005;94(1):61-76.
532 12. Ruan Y, Xu X, He Q, Li L, Guo J, Bao J, et al. The largest meta-analysis on the global prevalence of
533 microsporidia in mammals, avian and water provides insights into the epidemic features of these
534 ubiquitous pathogens. 2021;14(1):1-14.
535 13. Gumbo T, Sarbah S, Gangaidzo IT, Ortega Y, Sterling CR, Carville A, et al. Intestinal parasites in
536 patients with diarrhea and human immunodeficiency virus infection in Zimbabwe. 1999;13(7):819-821.
537 14. Widmer G, Akiyoshi DEJI, Genetics, Evolution. Host-specific segregation of ribosomal nucleotide
538 sequence diversity in the microsporidian Enterocytozoon bieneusi. 2010;10(1):122-128.
539 15. Didier ES, Khan IAJMPoO. The immunology of microsporidiosis in mammals. 2014:307-325.
540 16. Wei J, Fei Z, Pan G, Weiss LM, Zhou ZJFiM. Current therapy and therapeutic targets for
541 microsporidiosis. 2022;13.
542 17. Katiyar S, Gordon V, McLaughlin G, Edlind TJAa, chemotherapy. Antiprotozoal activities of
543 benzimidazoles and correlations with beta-tubulin sequence. 1994;38(9):2086-2090.
544 18. Horton JJP. Albendazole: a review of anthelmintic efficacy and safety in humans.
545 2000;121(S1):S113-S132.
546 19. Li J, Katiyar SK, Hamelin A, Visvesvara GS, Edlind TDJM, parasitology b. Tubulin genes from AIDS-
547 associated microsporidia and implications for phylogeny and benzimidazole sensitivity. 1996;78(1-
548 2):289-295.
549 20. Leder K, Ryan N, Spelman D, Crowe SMJSjoid. Microsporidial disease in HIV-infected patients: a
550 report of 42 patients and review of the literature. 1998;30(4):331-338.
551 21. Franzen C, Salzberger BJAa, chemotherapy. Analysis of the β-tubulin gene from Vittaforma
552 corneae suggests benzimidazole resistance. 2008;52(2):790-793.

553 22. Akiyoshi DE, Weiss LM, Feng X, Williams BA, Keeling PJ, Zhang Q, et al. Analysis of the β-Tubulin
554 Genes from Enterocytozoon bieneusi Isolates from a Human and Rhesus Macaque. 2007;54(1):38-41.
555 23. Armstrong EJJoIP. Fumidil B and benomyl: chemical control of Nosema kingi in Drosophila
556 willistoni. 1976;27(3):363-366.
557 24. Brooks W, Cranford J, Pearce LJJoIP. Benomyl: effectiveness against the microsporidian Nosema
558 heliothidis in the corn earworm, Heliothis zea. 1978;31(2):239-245.
559 25. Sakr SA, Samei HA, Soliman MJJMS. Exploring hepatotoxicity of benomyl: histological and
560 histochemical study on albino rats. 2004;4(1):77-83.
561 26. Barnes TB, Verlangieri AJ, Wilson MCJT. Reproductive toxicity of methyl-1-(butylcarbamoyl)-2-
562 benzimidazole carbamate (benomyl) in male Wistar rats. 1983;28(1-2):103-115.
563 27. Kotková M, Sak B, Hlásková L, Kváč MJEp. The course of infection caused by Encephalitozoon
564 cuniculi genotype III in immunocompetent and immunodeficient mice. 2017;182:16-21.
565 28. Lefkove B, Govindarajan B, Arbiser JLJEroa-it. Fumagillin: an anti-infective as a parent molecule
566 for novel angiogenesis inhibitors. 2007;5(4):573-579.
567 29. Sin N, Meng L, Wang MQ, Wen JJ, Bornmann WG, Crews CMJPotNAoS. The anti-angiogenic
568 agent fumagillin covalently binds and inhibits the methionine aminopeptidase, MetAP-2.
569 1997;94(12):6099-6103.
570 30. Han B, Weiss LMJEoott. Therapeutic targets for the treatment of microsporidiosis in humans.
571 2018;22(11):903-915.
572 31. Union ECJOJE. Commission Regulation (EU) No 37/2010 of 22 December 2009 on
573 pharmacologically active substances and their classification regarding maximum residue limits in
574 foodstuffs of animal origin. 2010;15(2377):1-72.
575 32. Troemel ER, Félix M-A, Whiteman NK, Barrière A, Ausubel FMJPb. Microsporidia are natural
576 intracellular parasites of the nematode Caenorhabditis elegans. 2008;6(12):e309.
577 33. Tamim El Jarkass H, Reinke AWJCM. The ins and outs of host-microsporidia interactions during
578 invasion, proliferation and exit. 2020;22(11):e13247.
579 34. Balla KM, Andersen EC, Kruglyak L, Troemel ERJPp. A wild C. elegans strain has enhanced
580 epithelial immunity to a natural microsporidian parasite. 2015;11(2):e1004583.
581 35. Balla KM, Luallen RJ, Bakowski MA, Troemel ERJNM. Cell-to-cell spread of microsporidia causes
582 *Caenorhabditis elegans* organs to form syncytia. 2016;1(11):1-6.
583 36. Willis AR, Zhao W, Sukhdeo R, Wadi L, El Jarkass HT, Claycomb JM, et al. A parental
584 transcriptional response to microsporidia infection induces inherited immunity in offspring.
585 2021;7(19):eabf3114.
586 37. El Jarkass HT, Mok C, Schertzberg MR, Fraser AG, Troemel ER, Reinke AWJE. An intestinally
587 secreted host factor promotes microsporidia invasion of C. elegans. 2022;11:e72458.
588 38. Reinke AW, Balla KM, Bennett EJ, Troemel ERJNc. Identification of microsporidia host-exposed
589 proteins reveals a repertoire of rapidly evolving proteins. 2017;8(1):14023.
590 39. Szumowski SC, Botts MR, Popovich JJ, Smelkinson MG, Troemel ERJPotNAoS. The small GTPase
591 RAB-11 directs polarized exocytosis of the intracellular pathogen *N. parisii* for fecal-oral transmission
592 from *C. elegans*. 2014;111(22):8215-8220.
593 40. Bojko J, Reinke AW, Stentiford GD, Williams B, Rogers MS, Bass DJTiP. Microsporidia: a new
594 taxonomic, evolutionary, and ecological synthesis. 2022.
595 41. Wadi L, El Jarkass HT, Tran TD, Islah N, Luallen RJ, Reinke AWJPp. Genomic and phenotypic
596 evolution of nematode-infecting microsporidia. 2023;19(7):e1011510.
597 42. Zhang G, Sachse M, Prevost M-C, Luallen RJ, Troemel ER, Felix M-AJPp. A large collection of
598 novel nematode-infecting microsporidia and their diverse interactions with Caenorhabditis elegans and
599 other related nematodes. 2016;12(12):e1006093.

43. Murareanu BM, Antao NV, Zhao W, Dubuffet A, El Alaoui H, Knox J, et al. High-throughput small molecule screen identifies inhibitors of microsporidia invasion and proliferation in C. elegans. 2022;13(1):5653.
44. Samby K, Besson D, Dutta A, Patra B, Doy A, Glossop P, et al. The pandemic response Box—Accelerating drug discovery efforts after disease outbreaks. 2022;8(4):713-720.
45. Shanley HT, Taki AC, Byrne JJ, Jabbar A, Wells TN, Samby K, et al. A high-throughput phenotypic screen of the 'Pandemic Response Box'identifies a quinoline derivative with significant anthelmintic activity. 2022;15(2):257.
46. Reader J, van der Watt ME, Taylor D, Le Manach C, Mittal N, Ottilie S, et al. Multistage and transmission-blocking targeted antimalarials discovered from the open-source MMV Pandemic Response Box. 2021;12(1):269.
47. Rice CA, Troth EV, Russell AC, Kyle DEJP. Discovery of anti-amoebic inhibitors from screening the MMV pandemic response box on Balamuthia mandrillaris, Naegleria fowleri, and Acanthamoeba castellanii. 2020;9(6):476.
48. Lewis JA, Fleming JTJMicb. Basic culture methods. 1995;48:3-29.
49. Hakim A, Mor Y, Toker IA, Levine A, Neuhof M, Markovitz Y, et al. WorMachine: machine learning-based phenotypic analysis tool for worms. 2018;16:1-11.
50. Vávra J, Ronny Larsson JJMpoo. Structure of microsporidia. 2014:1-70.
51. Willis AR, El Jarkass HT, Reinke AWJJ. Studying Inherited Immunity in a Caenorhabditis elegans Model of Microsporidia Infection. 2022;(182):e63636.
52. Fries I, Feng F, da Silva A, Slemenda SB, Pieniazek NJJEJoP. Nosema ceranae n. sp.(Microspora, Nosematidae), morphological and molecular characterization of a microsporidian parasite of the Asian honey bee Apis cerana (Hymenoptera, Apidae). 1996;32(3):356-365.
53. Lv Q, Zhou B, Liao H, He X, Chen Y, Pan G, et al. Proteomic profile of polar filament and polar tube from fungal pathogen microsporidium Nosema bombycis provides new insights into its unique invasion organelle. 2022;263:104617.
54. Labanauskas L, Brukštus A, Gaidelis P, Buchinskaite V, Udrenaite E, Daukšas VJPCJ. Synthesis and antiinflammatory activity of some new 1-acyl derivatives of 2-methylthio-5, 6-diethoxybenzimidazole. 2004;34(7):353-355.
55. Navarrete-Vázquez G, Hidalgo-Figueroa S, Torres-Piedra M, Vergara-Galicia J, Rivera-Leyva JC, Estrada-Soto S, et al. Synthesis, vasorelaxant activity and antihypertensive effect of benzo [d] imidazole derivatives. 2010;18(11):3985-3991.
56. Hosamani KM, Shingalapur RVJAdP. Synthesis of 2‐mercaptobenzimidazole derivatives as potential anti‐microbial and cytotoxic agents. 2011;344(5):311-319.
57. Hahnel SR, Zdraljevic S, Rodriguez BC, Zhao Y, McGrath PT, Andersen ECJPp. Extreme allelic heterogeneity at a Caenorhabditis elegans beta-tubulin locus explains natural resistance to benzimidazoles. 2018;14(10):e1007226.
58. Shaver AO, Wit J, Dilks CM, Crombie TA, Li H, Aroian RV, et al. Variation in anthelmintic responses are driven by genetic differences among diverse C. elegans wild strains. 2023;19(4):e1011285.
59. Gibson SB, Ness-Cohn E, Andersen ECJIJfPD, Resistance D. Benzimidazoles cause lethality by inhibiting the function of Caenorhabditis elegans neuronal beta-tubulin. 2022;20:89-96.
60. Dilks CM, Koury EJ, Buchanan CM, Andersen ECJIJfPD, Resistance D. Newly identified parasitic nematode beta-tubulin alleles confer resistance to benzimidazoles. 2021;17:168-175.
61. Poonam, Gupta Y, Gupta N, Singh S, Wu L, Chhikara BS, et al. Multistage inhibitors of the malaria parasite: Emerging hope for chemoprotection and malaria eradication. 2018;38(5):1511-1535.

645 62. Lim W, Nyuykonge B, Eadie K, Konings M, Smeets J, Fahal A, et al. Screening the pandemic
646 response box identified benzimidazole carbamates, Olorofim and ravuconazole as promising drug
647 candidates for the treatment of eumycetoma. 2022;16(2):e0010159.
648 63. Amato J, Iaccarino N, Pagano B, Morigi R, Locatelli A, Leoni A, et al. Bis-indole derivatives with
649 antitumor activity turn out to be specific ligands of human telomeric G-quadruplex. 2014;2:54.
650 64. Taha M, Uddin I, Gollapalli M, Almandil NB, Rahim F, Farooq RK, et al. Synthesis, anti-leishmanial
651 and molecular docking study of bis-indole derivatives. 2019;13:1-12.
652 65. Oh K-B, Mar W, Kim S, Kim J-Y, Lee T-H, Kim J-G, et al. Antimicrobial activity and cytotoxicity of
653 bis (indole) alkaloids from the sponge Spongosorites sp. 2006;29(3):570-573.
654 66. Mishra BB, Kale RR, Singh RK, Tiwari VKJF. Alkaloids: future prospective to combat leishmaniasis.
655 2009;80(2):81-90.
656 67. Tanaka J, Da Silva C, Ferreira I, Machado G, Leon L, De Oliveira AJP. Antileishmanial activity of
657 indole alkaloids from Aspidosperma ramiflorum. 2007;14(6):377-380.
658 68. Undeen AHJJoTB. A proposed mechanism for the germination of microsporidian (Protozoa:
659 Microspora) spores. 1990;142(2):223-235.
660 69. Willis AR, Reinke AW. Factors That determine Microsporidia infection and host specificity.
661 Microsporidia: Current Advances in Biology: Springer; 2022. p. 91-114.
662 70. Weidner E, Byrd WJTJocb. The microsporidian spore invasion tube. II. Role of calcium in the
663 activation of invasion tube discharge. 1982;93(3):970-975.
664 71. Pleshinger J, Weidner EJTJocb. The microsporidian spore invasion tube. IV. Discharge activation
665 begins with pH-triggered Ca2+ influx. 1985;100(6):1834-1838.
666 72. UNDEEN AH, FRIXIONE EJTJoP. The role of osmotic pressure in the germination of nosema
667 algerae spores 1. 1990;37(6):561-567.
668 73. Dang X, Pan G, Li T, Lin L, Ma Q, Geng L, et al. Characterization of a subtilisin-like protease with
669 apical localization from microsporidian Nosema bombycis. 2013;112(2):166-174.
670 74. Wang R, Li Q, Liu F, Dang X, Sun Q, Sheng X, et al. Maturation of subtilisin-like protease NbSLP1
671 from microsporidia Nosema bombycis. 2022:1126.
672 75. Mead JR, McNair NJFML. Antiparasitic activity of flavonoids and isoflavones against
673 Cryptosporidium parvum and Encephalitozoon intestinalis. 2006;259(1):153-157.
674 76. Dhanak D, Keenan RM, Burton G, Kaura A, Darcy MG, Shah DH, et al. Benzothiopyran-4-one
675 based reversible inhibitors of the human cytomegalovirus (HCMV) protease. 1998;8(24):3677-3682.
676 77. Cowell AN, Istvan ES, Lukens AK, Gomez-Lorenzo MG, Vanaerschot M, Sakata-Kato T, et al.
677 Mapping the malaria parasite druggable genome by using in vitro evolution and chemogenomics.
678 2018;359(6372):191-199.
679 78. Didier PJ, Phillips JN, Kuebler DJ, Nasr M, Brindley PJ, Stovall ME, et al. Antimicrosporidial
680 activities of fumagillin, TNP-470, ovalicin, and ovalicin derivatives in vitro and in vivo. 2006;50(6):2146-
681 2155.

682